

Experimental overview of correlations in small collision systems

A brief history

Soumya Mohapatra^{1,*}

¹*Department of Physics, Columbia University*

Abstract. The azimuthal anisotropies of particle yields observed in relativistic heavy ion collisions have been traditionally considered as a strong evidence of the formation of a deconfined quark-gluon plasma in these collisions. However multiple recent measurements in pp and $p/D/He+A$ collisions show similar features as those observed in heavy ion collisions, indicating the possibility of the production of such a deconfined medium in smaller collision systems. This paper presents a comprehensive summary of such measurements in small systems. It includes measurements of identified and inclusive two-particle correlations in $\Delta\phi$ and $\Delta\eta$, with different procedures used to subtract the dijet contributions, as well as measurements of multi-particle cumulants $c_n\{2-8\}$. The traditional cumulant measurements confirm presence of collective phenomena in $p+A$ collisions, but are biased by non-flow correlations and are not able to provide evidence for collectivity in pp collisions. To address this, a new subevent cumulant method that further suppresses the contribution non-flow effects was developed, whose measurements are also discussed.

1 Introduction

In relativistic heavy ion collisions, such as those at the RHIC and at the LHC, the colliding nuclei are heated to high enough temperatures such that the quarks and gluons that are ordinarily confined within nucleons get de-localized and a new state of matter called the quark-gluon plasma (QGP) is created. The medium expands anisotropically driven the pressure gradients between the medium and the outside vacuum, cooling down as it expands and finally hadronizes. The final particle yields in the azimuthal (ϕ) direction are typically parameterized as a Fourier series [1]:

$$dN/d\phi \propto (1 + 2 \sum v_n \cos n(\phi - \Psi_n)), \quad (1)$$

where the v_n and Ψ_n denote the magnitude and orientation of the single-particle anisotropies. Due to their hydrodynamic origin in heavy ion collisions, the v_n are often called flow harmonics.

Such azimuthal anisotropies were not expected to arise in proton-proton (pp) and proton-nucleus ($p+A$) collisions where the QGP was not expected to be formed. However in 2010 the CMS collaboration showed that in high-multiplicity pp collisions, two-particle correlations (2PCs) in relative azimuthal angle ($\Delta\phi=\phi^a - \phi^b$) and pseudorapidity separation ($\Delta\eta=\eta^a - \eta^b$), where the superscripts a and b label the two particles used in the correlation, showed the presence of a long range correlation structure along $\Delta\eta$ at $\Delta\phi \sim 0$ [2]. This structure, commonly called “ridge”, is also seen in heavy ion

*e-mail: soumya@cern.ch

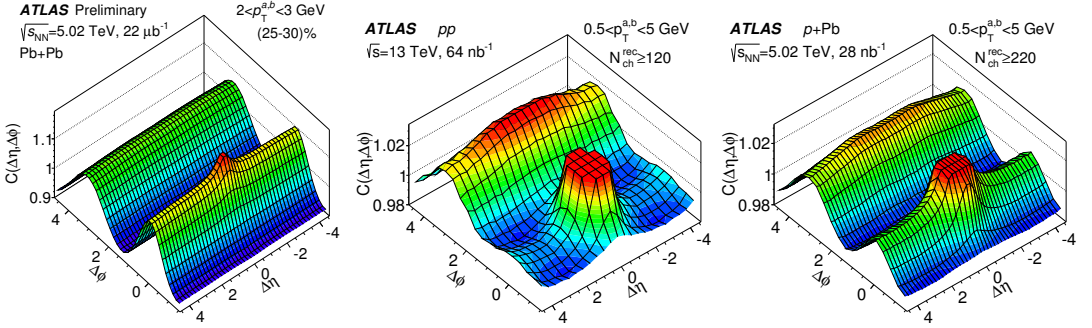


Figure 1. Two particle correlations ($C(\Delta\eta, \Delta\phi)$) in Pb+Pb(left), pp (center) and $p+Pb$ (right) collisions. The Pb+Pb results are for $2 < p_T^{a,b} < 3$ GeV and for the 25–30% centrality interval. The pp results are for $0.5 < p_T^{a,b} < 5$ GeV and for events having more than 120 reconstructed charged particles with $p_T > 0.4$ GeV. The $p+Pb$ results are for $0.5 < p_T^{a,b} < 5$ GeV and for events having more than 220 reconstructed charged particles with $p_T > 0.4$ GeV. The plots are from Refs. [4, 5]

collisions and arises there due to collective flow. Thus its presence in pp collisions indicated the possibility of collective effects being present in pp collisions. The left and middle panels of Figure 1 compare the ridge seen in Pb+Pb and pp collisions, respectively. The pp ridge is seen to be considerably weaker than the Pb+Pb ridge. The weakness of the ridge in pp collisions made it impossible to use the techniques that were developed for and used in analysis of 2PCs in A+A collisions. Furthermore, the pp -ridge could be explained by initial state models based on gluon saturation [3], and this was accepted by the heavy ion community as its origin.

2 Collectivity in $p+A$ collisions

In 2012 the analysis of the first $p+Pb$ collision data at the LHC from ATLAS, ALICE and CMS collaborations showed the presence of the ridge in $p+Pb$ collisions as well [6–10]. Unlike the pp case, the long-range correlations in $p+Pb$ were strong enough (see Figure 1 right panel), and the multiplicities were large enough, that the techniques used for analysis of 2PCs in A+A collisions could be applied. The 2PC analysis indicated that the long-range correlations were indeed arising from single-particle anisotropies, v_n , which could be extracted using the 2PCs [7]. The $p+Pb$ - v_n were found to be remarkably similar to than seen in A+A collisions. In fact, after some trivial scalings, the v_2 – v_4 in $p+Pb$ had exactly the same p_T dependence as the v_n in Pb+Pb collisions [9]. This is demonstrated in Figure 2. The left panels show the comparison of v_2 – v_4 as a function of p_T in Pb+Pb and $p+Pb$ collisions. The centrality interval of 55–60% in the Pb+Pb data is chosen such that it approximately corresponds to the multiplicity range of the $p+Pb$ data to which it is compared ($220 \leq N_{ch}^{rec} < 260$). The right panels of Figure 2, the Pb+Pb data are rescaled horizontally by a constant factor of 1.25, and the v_2 and v_4 are also down-scaled by an empirical factor of 0.66 to match the $p+Pb$ data. The factor of 1.25 is to account for the difference in the $\langle p_T \rangle$ between the Pb+Pb and $p+Pb$ data [11], while the empirical factor of 0.66 accounts for the differences in the collision geometry in the two systems.

Additionally, measurement of v_n via multi-particle cumulants and Lee-Yang Zeroes (LYZ) methods in $p+Pb$ collisions also exhibited similarities with Pb+Pb collisions [10]. Figure 3 shows the v_2 obtained from 4, 6 and 8-particle cumulants ($v_2\{4\}$, $v_2\{6\}$) together with the v_2 from 2PCs ($v_2\{2, \Delta\eta > 2\}$)

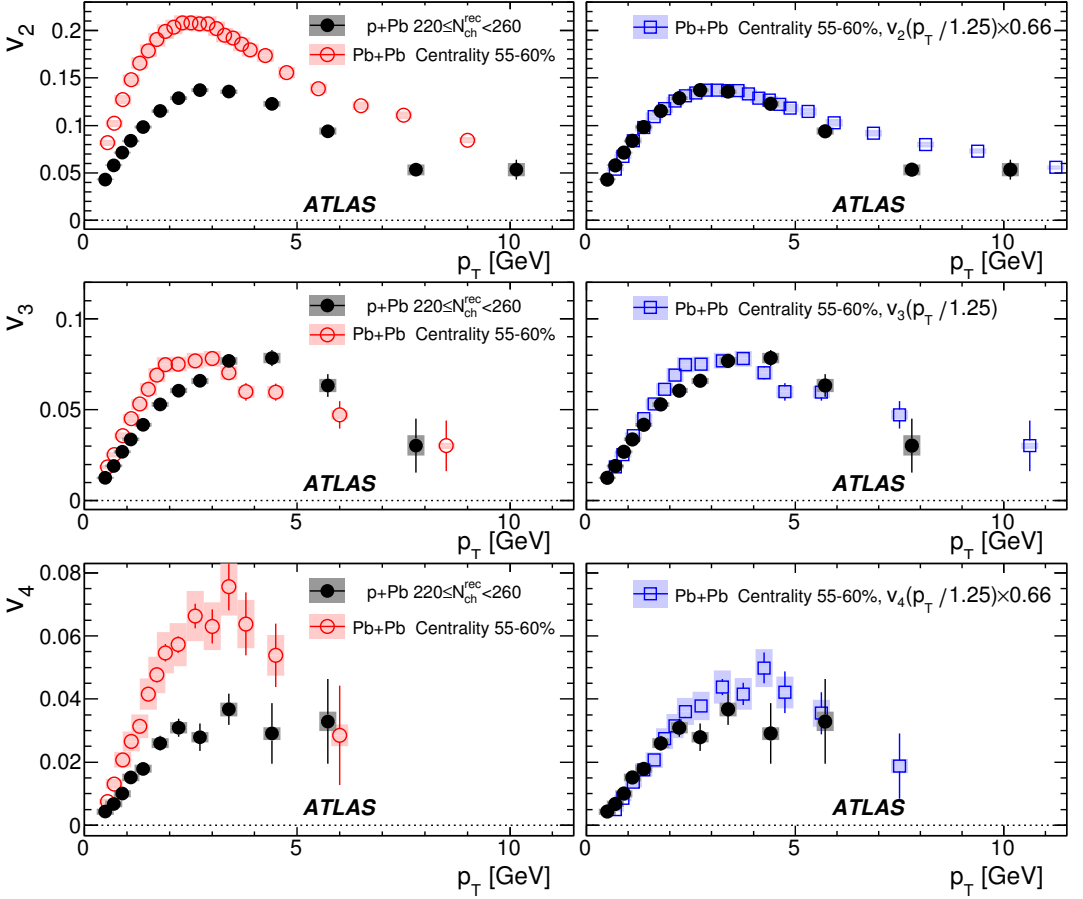


Figure 2. The coefficients v_2 (top row), v_3 (middle row) and v_4 (bottom row) as a function of p_T compared between p +Pb collisions with $220 \leq N_{ch}^{rec} < 260$ and Pb+Pb collisions in 55–60% centrality. The left column shows the original data with their statistical (error bars) and systematic uncertainties (shaded boxes). In the right column, the same Pb+Pb data are rescaled horizontally by a constant factor of 1.25, and the v_2 and v_4 are also down-scaled by an empirical factor of 0.66 to match the p +Pb data. The Figures are taken from Ref. [9].

in Pb+Pb (left) and p +Pb collisions (right). It is seen that in both systems, the v_2 obtained from the 4, 6 and 8 particle cumulants are identical within systematic uncertainties, and smaller than the 2PC- v_2 . This ordering of the v_2 measured via these different methods is considered a characteristic of flow phenomena [10].

Further more, v_n measurements in other small-large collision systems, namely d +A and ^3He +A collisions, also demonstrated similarities with A+A collisions, and were well reproduced by hydrodynamic calculations [12–16]. A summary of such results from the PHENIX collaboration is shown in Figure 4. These and other measurements established with considerable certainty the presence of collective behavior in p /D/He+A collisions.

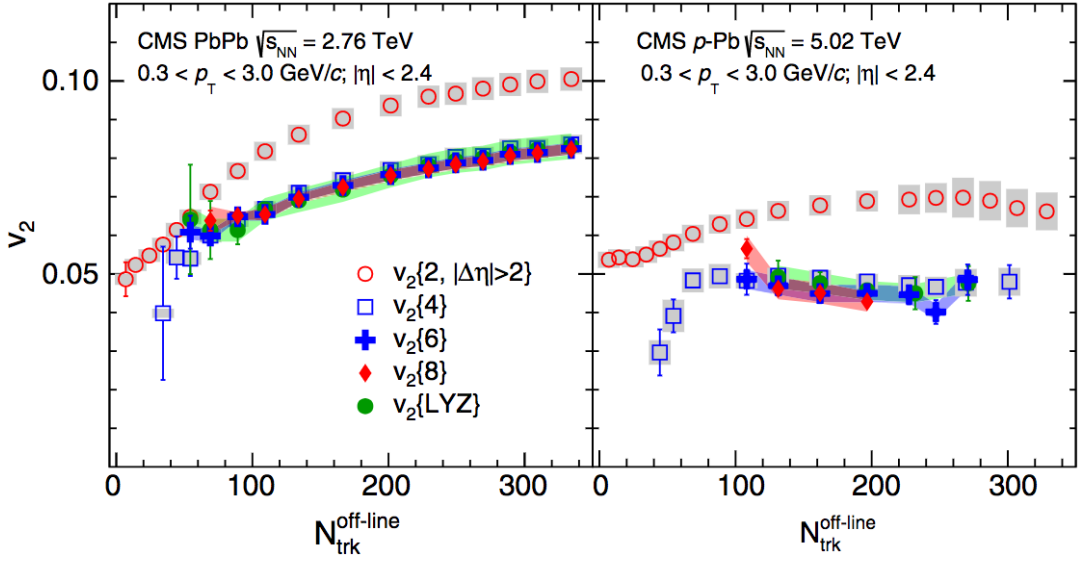


Figure 3. The multiplicity dependence of the v_2 obtained from 2PCs ($v_2\{2, \Delta\eta > 2\}$), from 4, 6 and 8-particle cumulants ($v_2\{4\}$, $v_2\{6\}$ and $v_2\{8\}$), and from Lee-Yang Zeroes (LYZ) methods. Results are for particles with $0.3 < p_T < 3$ GeV. The left panel corresponds to Pb+Pb collisions with $\sqrt{s_{NN}}=2.76$ TeV. The right panel corresponds to p+Pb collisions with $\sqrt{s_{NN}}=5.02$ TeV. The error bars and bands indicate statistical and systematic uncertainties, respectively. Figure taken from Ref. [10].

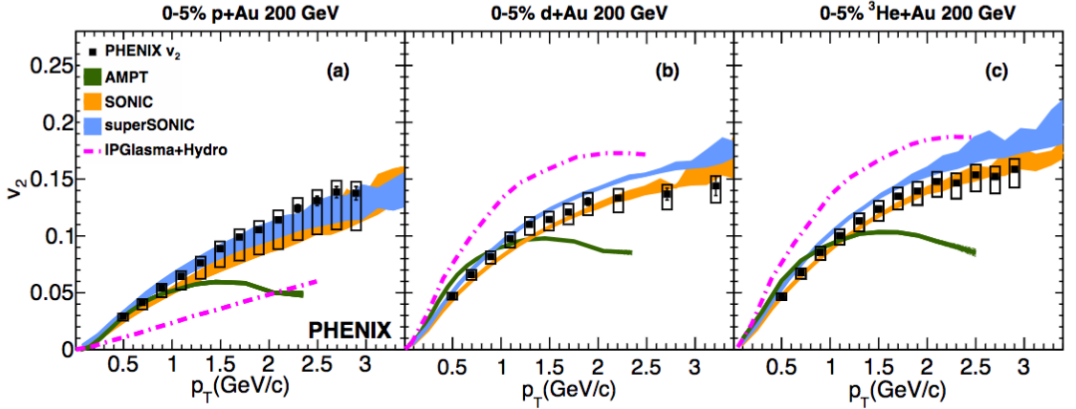


Figure 4. The p_T dependence of the v_2 measured in 0–5% most central p+Au (left), D+Au (center) and $^3\text{He} + \text{Au}$ collisions at $\sqrt{s_{NN}}=200$ GeV. Also shown on the plots are theoretical calculations from the AMPT, SONIC, superSONIC and IPGlasma+Hydro. Figure taken from [16].

3 Long-range correlations in pp collisions

These measurements thus necessitated revisiting the pp long-range correlations to perform a more detailed analysis along the lines of the p +Pb measurements and extract the v_n harmonics. However unlike the p +Pb measurements, the long-range correlation in pp collisions are much weaker compared to the other features seen in the 2PC, namely, the near-side jet peak at $\Delta\eta, \Delta\phi \sim (0,0)$, and the away-side jet correlation at $\Delta\phi \sim \pi$. The near-side peak can be removed by focussing on the 1D correlation, $C(\Delta\phi)$, obtained by projecting the long-range ($|\Delta\eta| > 2$) part of the correlation on to the $\Delta\phi$ -axis. This is shown in the left panel of Figure 5 for pp events at $\sqrt{s}=13$ TeV, that have more than 120 reconstructed charged particle tracks with $p_T > 0.4$ GeV ($N_{\text{ch}}^{\text{rec}}$). While the $\Delta\eta$ cut removes the near-side peak, the away-side jet peak still remains and dominates the 2PC, and must be somehow removed, prior to extracting the v_n from the correlation functions. This was recently done by the ATLAS collaboration who performed a ‘‘Template-fit’’ procedure to remove the contribution of the away-side jet to the 1D 2PC [5, 17]. In this procedure, the measured $C(\Delta\phi)$ distributions are assumed to result from a superposition of a ‘‘peripheral’’ $C(\Delta\phi)$ distribution, $C^{\text{periph}}(\Delta\phi)$, scaled up by a multiplicative factor and a constant modulated by $\cos(n\Delta\phi)$ for $n \geq 2$. The resulting template fit function,

$$C^{\text{templ}}(\Delta\phi) = C^{\text{ridge}}(\Delta\phi) + F C^{\text{periph}}(\Delta\phi), \quad (2)$$

where

$$C^{\text{ridge}}(\Delta\phi) = G \left(1 + \sum_{n=2}^{\infty} 2v_{n,n} \cos(n\Delta\phi) \right), \quad (3)$$

has free parameters F and $v_{n,n}$. The parameter F is the multiplicative factor by which the $C^{\text{periph}}(\Delta\phi)$ is scaled. The coefficient G , which represents the magnitude of the combinatoric component of $C^{\text{ridge}}(\Delta\phi)$, is fixed by requiring that the integral of $C^{\text{templ}}(\Delta\phi)$ be equal to the integral of the measured $C(\Delta\phi)$: $\int_0^\pi d\Delta\phi C^{\text{templ}}(\Delta\phi) = \int_0^\pi d\Delta\phi C(\Delta\phi)$. In the ATLAS analysis, the $0 \leq N_{\text{ch}}^{\text{rec}} < 20$ multiplicity interval is used to produce $C^{\text{periph}}(\Delta\phi)$. The right panel of Figure 5 shows an example of the template fitting for the $N_{\text{ch}}^{\text{rec}} > 120$ multiplicity interval. It is seen that the template describes the data quite well, reproducing both the near-side ridge as well as the narrowing of the away-side peak from low- $N_{\text{ch}}^{\text{rec}}$ to high- $N_{\text{ch}}^{\text{rec}}$ events.

Once the long-range correlation is extracted from the template fits, the single-particle anisotropies v_n can be extracted, following the standard procedure used in heavy ion analyses [1], where the Fourier coefficients $v_{n,n}$ of the 2PC (Eq. (3)) are related to the v_n as:

$$v_{n,n}(p_T^a, p_T^b) = v_n(p_T^a, p_T^b). \quad (4)$$

The left panel of Figure 6 shows the v_2 in 13 TeV and 5.02 TeV pp collisions obtained from the template fits. Also shown for comparison are the v_2 values in p +Pb collisions at $\sqrt{s_{\text{NN}}}=5.02$ TeV. Very interestingly it is observed that the pp v_2 is independent of $N_{\text{ch}}^{\text{rec}}$, implying that the long range correlation is not a feature that is unique to high multiplicity events only, but in fact is present at all multiplicities. The p +Pb v_2 does show a dependence on $N_{\text{ch}}^{\text{rec}}$ and is always larger than the pp v_2 , possibly arising from geometrical effects that are present in p +Pb but not in pp collisions. However, at the lowest multiplicities the p +Pb v_2 values seem to approach the pp v_2 values. Another feature that is observed is that the pp v_2 values at 5.02 and 13 TeV are consistent with each other, implying a collision energy independence of the pp v_2 similar to what is observed in A+A collisions [4, 18]. The right panel of Figure 6 shows the v_2 as a function of p_T , for the same three datasets. As seen in the $N_{\text{ch}}^{\text{rec}}$ dependence, the v_2 values are consistent between the 5.02 and 13 TeV pp within the systematic uncertainties, over the measured p_T range. The pp v_2 values are smaller than the p +Pb v_2 across

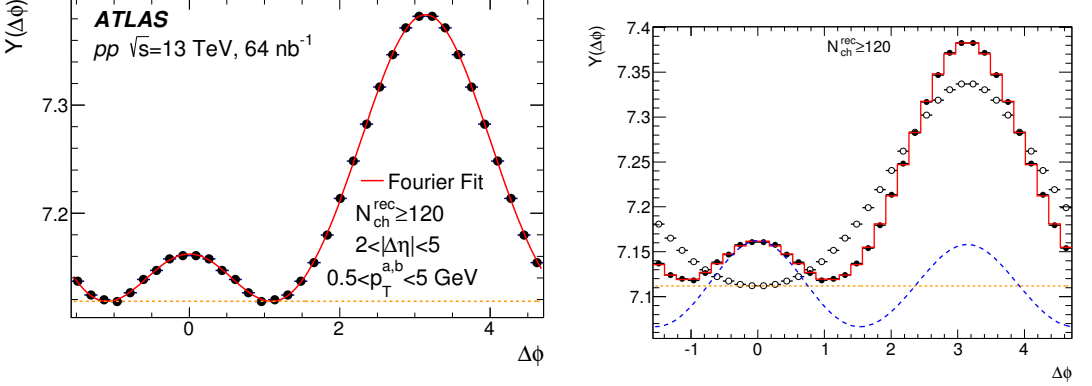


Figure 5. Left panel : The 1D two-particle correlation, in pp events at $\sqrt{s}=13$ TeV. The 1D correlations are obtained by projecting the long range ($\Delta\eta > 2$) part of the 2PC to $\Delta\phi$. The plot is for events with more than 120 reconstructed tracks, and for $0.5 < p_T^a, p_T^b < 5.0$ GeV. The continuous line is drawn only to guide the eye. Right panel: Template fit to the 1D 2PC. The template fitting includes second-order, third-order and fourth-order harmonics. The solid points indicate the measured 2PC, the open points and curves show different components of the template (see legend). The Figures are taken from Ref. [5].

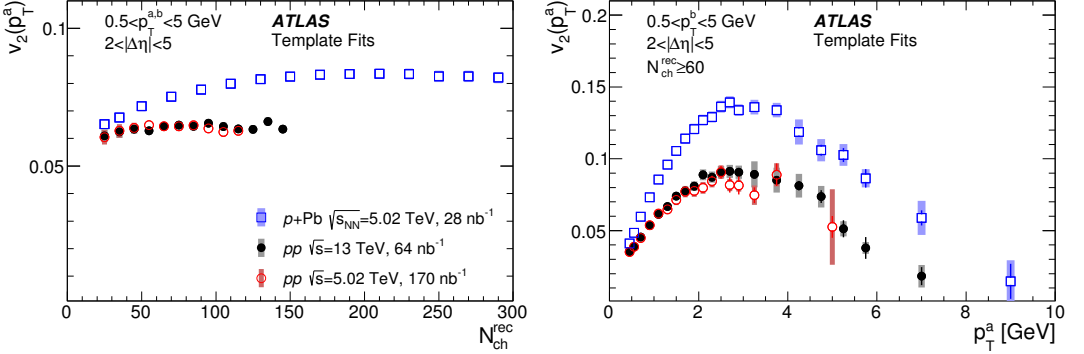


Figure 6. Left panels: comparison of the v_2 obtained from the template fitting procedure in the 13 TeV pp , 5.02 TeV pp , and 5.02 TeV $p+Pb$ data, as a function of N_{ch}^{rec} . The results are for $0.5 < p_T^a, p_T^b < 5$ GeV. Right panels: the p_T dependence of the v_2 for the $N_{ch}^{rec} \geq 60$ multiplicity range. The error bars and shaded bands indicate statistical and systematic uncertainties, respectively. The Figures are taken from Ref. [5].

the whole p_T range. However the shapes of the $v_2(p_T)$ are quite similar between the pp and $p+Pb$ collisions. This is seen in Figure 7 where the pp v_2 is scaled by an empirical factor of 1.51, chosen such that the maxima of the two $v_2(p_T)$ match. This similarity between the v_2 in these two systems, and by extension to the v_2 in A+A (see Figure 2) again suggests similar origin for the v_n in the three systems.

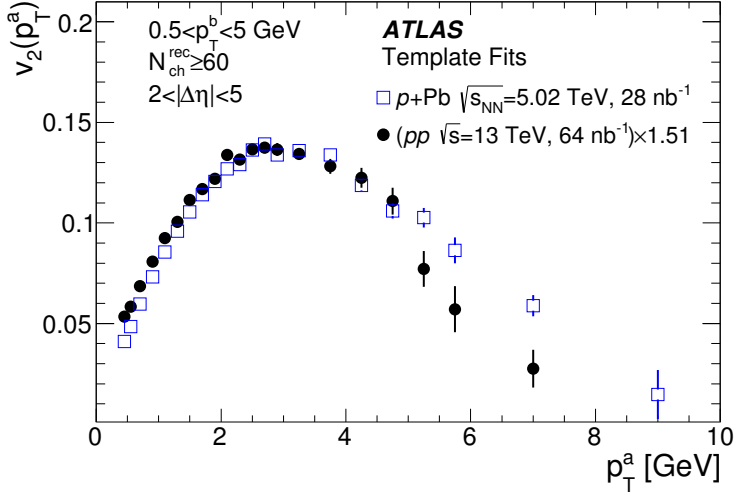


Figure 7. Comparison of the shapes of the $v_2(p_T)$ in 13 TeV pp and 5.02 TeV $p+Pb$ data. The pp v_2 has been scaled by a factor of 1.51 along the y -axis in order to match the maximum of the v_2 in the two data sets. The results are for $N_{ch}^{rec} \geq 60$. The error bars indicate statistical uncertainties. The Figures are taken from Ref. [5].

Besides two-particle correlations, multi-particle cumulants [19] have also been extensively used in A+A and $p+A$ collisions [20–22] to measure the v_n . The n -particle cumulant suppresses non-flow correlations involving n or fewer particles, and is very effective in involving non-flow azimuthal correlations in A+A and $p+A$ collisions, as the non-flow correlations (such as those arising from jets, decays etc.) that only correlate few-particles among themselves. Thus it is natural to use the multi-particle cumulants in pp collisions to study azimuthal anisotropies. However, the multiplicities in pp collisions are so small that despite the suppression of such few particle correlations, they still affect the measured v_n . This inadequacy of the cumulants in measuring the v_n in pp collisions was recently demonstrated in Ref. [23], where the authors showed that the cumulants give significant and large non-zero values when analyzing MC events generated with the PYTHIA-8 [24] event generator. The authors of Ref. [23] proposed improved cumulant methods, called two-subevent and three-subevent cumulants, where the particles used in the cumulants are taken from two and three different η regions, respectively. This η separation, further suppresses jet-like correlations. Recently the ATLAS collaboration performed such subevent cumulant measurements in pp collisions [25]. Figure 8 shows the multiplicity dependence of the three-subevent $v_2\{4\}$ measured in 5.02 TeV and 13 TeV pp collisions (left and middle panels) and compares them to the $v_2\{4\}$ seen in 5.02 TeV $p+Pb$ collisions (right panel). Also shown for comparison are the v_2 values obtained from the 2PCs. It is seen that the ordering $v_2\{2PC\} > v_2\{4\}$ is observed in pp collisions just as it was observed in the $p+Pb$ and $Pb+Pb$ (Figure 3) collisions, again giving indications of collectivity in pp collisions.

4 Summary

The measurement of long-range correlations in $p/D/He+A$ collisions and their similarity to A+A collisions is quite striking and has established the presence of collective phenomena in such systems. Analysis of collectivity via measurement of the long-range correlation in pp collisions is considerably more

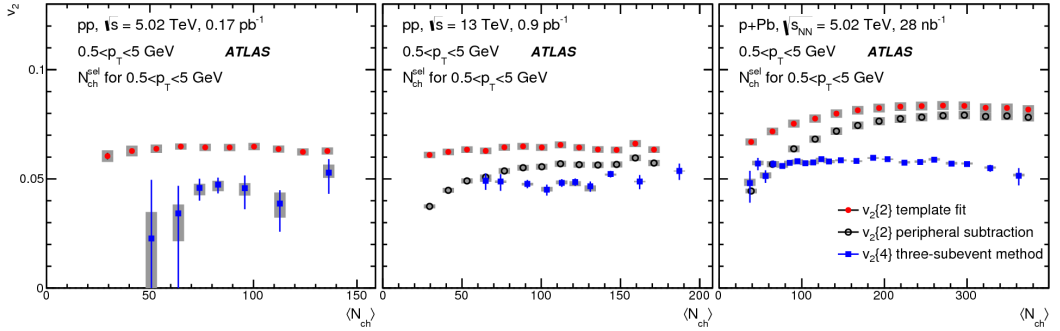


Figure 8. The $v_2\{4\}$ values calculated for charged particles with $0.5 < p_T < 5$ GeV using the three-subevent method in 5.02 TeV pp (left panel), 13 TeV pp (middle panel) and 5.02 TeV $p+Pb$ collisions (right panel). They are compared to the v_2 obtained from the 2PC analyses where the non-flow effects are removed by a template fit procedure (solid circles). Figure adapted from Ref. [25].

challenging. As described above, the most critical step in analyzing the long-range correlations in pp collisions is the removal of correlations arising from jets and dijets. The standard cumulants that work quite well in A+A collisions fail in pp collisions, as demonstrated in Ref. [25]. The subevent cumulants and template fitting procedure provide two effective methods of removing the jet and dijet correlations. However, even in these two methods, there might still be residual correlations from jets and dijets left over, so the results still must be taken with a pinch of salt. From the measurement, there are strong indications that global correlations - those that involve most of the particles produced in an event - are present in pp collisions. These correlations quantified by the Fourier coefficients v_n , demonstrate no dependence on the collision energy over \sqrt{s} of 2.76–13 TeV, similar to the $\sqrt{s_{NN}}$ independence of the v_n seen in A+A collisions. The correlations show no dependence on the multiplicity of the pp collision either, i.e. they are just as strong in low-multiplicity events as they are in high multiplicity events. The subevent cumulant measurements show that the $v_2\{2\}$ is larger than $v_2\{4\}$, similar to that seen in A+A collisions, indicating the presence of event-by-event v_2 fluctuations. Furthermore, the p_T dependence of the v_2 seen in pp collisions is qualitatively similar to that seen in $p+A$ and A+A collisions, in fact up to an overall scaling the $v_2(p_T)$ look identical between pp , $p+Pb$ and A+A collisions. All these observations give strong indications of collective behavior in pp collisions.

Acknowledgments

This work was supported by the US Department of Energy Office of Science, Office of Nuclear Physics under Award No. DE-FG02-86ER40281.

References

- [1] ATLAS Collaboration, Phys. Rev. C **86**, 014907 (2012)
- [2] CMS Collaboration, JHEP **1009**, 091 (2010)
- [3] A. Dumitru, K. Dusling, F. Gelis, J. Jalilian-Marian, T. Lappi, R. Venugopalan, Phys. Lett. B **697**, 21 (2011)

- [4] ATLAS Collaboration, ATLAS-CONF-2016-105 (2016)
- [5] ATLAS Collaboration, Phys. Rev. **C96**, 024908 (2017), 1609.06213
- [6] ALICE Collaboration, B. Abelev et al., Phys. Lett. B **719**, 29 (2013)
- [7] ATLAS Collaboration, Phys. Rev. Lett. **110**, 182302 (2013)
- [8] CMS Collaboration, Phys. Lett. B **724**, 213 (2013)
- [9] ATLAS Collaboration, Phys. Rev. C **90**, 044906 (2014)
- [10] CMS Collaboration, Phys. Rev. Lett. **115**, 012301 (2015)
- [11] G. Başar, D. Teaney, Phys. Rev. C **90**, 054903 (2014)
- [12] PHENIX Collaboration, A. Adare et al., Phys. Rev. Lett. **111**, 212301 (2013)
- [13] PHENIX Collaboration, A. Adare et al., Phys. Rev. Lett. **114**, 192301 (2015)
- [14] STAR Collaboration, L. Adamczyk et al., Phys. Lett. B **747**, 265 (2015)
- [15] PHENIX Collaboration, A. Adare et al., Phys. Rev. Lett. **115**, 142301 (2015)
- [16] PHENIX Collaboration, C. Aidala et al. , Phys. Rev. **C95**, 034910 (2017)
- [17] ATLAS Collaboration, Phys. Rev. Lett. **116**, 172301 (2016)
- [18] ALICE Collaboration, A. Jaroslav et al., Phys. Lett. **B762**, 376 (2016)
- [19] N. Borghini, P.M. Dinh, J.Y. Ollitrault, Phys. Rev. **C63**, 054906 (2001)
- [20] ATLAS Collaboration, Eur. Phys. J. C **74**, 3157 (2014)
- [21] ATLAS Collaboration, Phys. Lett. B **725**, 60 (2013)
- [22] ALICE Collaboration, Phys. Rev. Lett. **105**, 252302 (2010)
- [23] J. Jia, M. Zhou, A. Trzupek, Phys. Rev. **C96**, 034906 (2017)
- [24] T. Sjöstrand, S. Mrenna, P.Z. Skands, Comput. Phys. Commun. **178**, 852 (2008)
- [25] ATLAS Collaboration (2017), arXiv 1708.03559